Int. J. Wildland Fire 5(3): 173-192, 1995
© IAWF. Printed in U.S.A.

Calibration of a Large Fuel Burnout Model

Frank A. Albini[1], James K. Brown[2], Elizabeth D. Reinhardt[3], and Roger D. Ottmar[4]

[1]*Mechanical Engineering Department, Montana State University, Bozeman, Montana 59717*
Tel. 406 994 6298; Fax 406 994 6292; e-mail umefa@msu.oscs.montana.edu

[2] *Intermountain Fire Sciences Laboratory, PO Box 8089, Missoula, Montana 59807*
Tel. 406 329 4803; Fax 406 329 4877; e-mail fswa/s=J.Brown/ou1=s22L01A@mhs.attmail.com

[3] *Intermountain Fire Sciences Laboratory, PO Box 8089, Missoula, Montana 59807*
Tel. 406 329 4836; Fax 406 329 4877; e-mail fswa/s=E.Reinhardt/ou1=s22L01A@mhs.attmail.com

[4]*Forestry Sciences Laboratory, 4043 Roosevelt Way, NE, Seattle, Washington 98105*
Tel. 206 553 7815; Fax 206 553 7709; e-mail fswa/s=R.Ottmar/ou1=r06F05A@mhs.attmail.com

Abstract. A computer simulation of the burning of large woody natural fuels has been created. The model simulates flaming combustion of large woody surface fuels but includes the influence of smoldering duff on this burning. This paper describes calibration of empirical constants in the model using data from laboratory crib burns and from prescribed burns in harvest debris and in natural fuel accumulations. The calibrated model reproduced laboratory crib burning rates and natural fuel loading reductions with acceptable accuracy.

Keywords: Fuel reduction; heat release; intensity; burning rate

Introduction

It has long been recognized that the process of fire spread in wildland fuels is largely controlled by those fuel components with the largest surface/volume ratios (Brown and Davis 1973, Luke and MacArthur 1977, Chandler et al 1983). Because of the dominant importance of the finest fuels in controlling spread rate, modelers of wildland fire behavior have focused on these components almost exclusively (Rothermel 1972, Grishin 1981, 1992, Albini 1986). But in assessing the effects of a wildland fire it is often more important to be able to predict the amount of duff consumed or the rate and amount of consumption of large woody fuels than to predict the speed with which an igniting surface fire would propagate over the burn site.

Most studies of the quantity of consumption of duff and of large woody fuels have been empirical in nature (see recent summary in Brown, Reinhardt and Fischer 1991) and serve well the purpose of predicting fuel quantity reduction. But occasions arise when one desires to predict the rate of heat release from burning of large woody fuels. Such predictions might be used for estimating the rate of heat transfer to the soil (Hungerford 1990) or the maximum distance of potential spot fires (Albini 1981). In this case one must turn either to correlations of the burning rates of compartments and wood cribs (Harmathy 1972ab, Drysdale 1985, Anderson 1990) or to a suspect model for the burnout of natural fuels based mostly on conjecture (Albini 1976).

Collaborative research addressing this deficiency is currently under way, involving USDA Forest Service personnel at the Intermountain Fire Sciences Laboratory in Missoula, Montana and the Mechanical Engineering Department at Montana State University in Bozeman, Montana. The objective of this research is creation of a model for the rate of burning of large woody natural fuels based more firmly upon physical process models and making use of field burn data from several sources to calibrate empirical factors. This paper reports calibration of empirical constants used in the model to control the rate of fuel burning and the quantity of large woody surface fuel consumed. The roles of the empirical parameters are explained more fully in the overviews of process simulation and model structure below.

Overview of Process Simulation

The simulation that has been constructed attempts to approximate the physical processes involved in the burning of large woody natural fuels not with the precision that would be needed in the simulation of an

industrial combustion process, but with enough realism to assure sensitivity of model predictions to parameters widely recognized to be important.

For example, the burning rate of any given fuel element is greater when it is thrust into a fiercely burning furnace than when it is simply kindled with a few smaller burning elements. And in either environment its burning rate decreases as its moisture content increases. These sensitivities are assured by modeling the rate of burning of a fuel element as being proportional to the rate at which heat is transferred to the element and inversely proportional to the heat required to raise a unit volume of it to the temperature at which it is converted to char. This crude approximation of the solid fuel combustion process is used in the model discussed here.

The simplest model for the rate of heat transfer to a fuel element from its environment, known as a Newtonian film heat transfer model (Incropera and DeWitt 1985), is that the rate is proportional to the difference between the temperature of the environment and the temperature of the fuel element's surface. We represent the heating environment experienced by a fuel element in terms of a "fire environment temperature". This term represents the equilibrium temperature that would be achieved by an inert object of roughly the same size and surface character as the fuel element if it were to reside for a long enough time in an unchanging environment the same as that being experienced by the fuel element at the instant considered. The representation of this quantity in terms of the local rate of heat release per unit ground area (i.e. the local fire intensity) and the proximity of burning neighbor elements involves empirical parameters whose values influence the prediction of burning rate.

Mathematical completeness, or "closure", of the model is achieved by summing up the rates at which all the fuel elements are burning to obtain the total rate of heat release per unit area of the burn site. In forming this sum, we examine each fuel size class in terms of the degree to which it interacts with other fuel elements of the same size and smaller.

This is done to allow accomodation of the fact that, at any moment, some small size classes may have been completely burned up, larger ones may be burning, and even larger ones may not yet be ignited. In such a situation, some components of a given size class will be experiencing a fire intensity that is more or less than the site-average fire intensity, and this variation can be accounted for.

Description of the interaction of fuel elements involves an empirical parameter whose value selection is described below. Note that it is necessary to consider only "the same and smaller sizes" to avoid double counting of fuel size classes. The model uses the oversimplification that the burning rate of a given size class is influenced by the burning of size classes larger than its own only through the contribution of the larger elements to the site-average fire intensity. Fuel elements that do not interact with any other surface fuel elements are assumed to be exposed to or resting upon the surface of the burn site, so experience a fire intensity given by the sum of the site-average fire intensity due to the burning of all surface fuels plus the intensity contributed by the burning of duff, if any.

The following sections give technical details of inputs to the model, describe more explicitly the mathematical algorithms, and identify the empirical parameters whose values are determined by matching model predictions to data. Those not interested in such details may wish to skip to the sections on calibration and testing.

Overview of Model Structure

The model exists in the form of a set of computer algorithms implementing a time-based simulation with multiple event-based branches. The code runs on a personal computer in an interactive mode, with user input prompted and menu aided. The algorithms are conceptually simple and their operations can be broadly outlined briefly (Albini 1994) but a detailed description of the sequence of steps in some parts of the model devolves to a reading of the FORTRAN source code. We strive here for a balance between thoroughness and tedium.

Input to the model is a complete description of the fuel on the burn site, some parameters that control the operation and performance of the model, and some environmental variables that are necessary for completeness but are not important in determining the model predictions. To facilitate repeated model exercises, data files can be archived and retrieved as fuel description packages and as environmental and program-control packages. SI (metric) units are used for both input and output.

Each surface fuel category is described by a unique alphanumeric name, its loading (dry mass per unit area, kg/m^2), surface/volume ratio, m^{-1}, and moisture mass fraction, as well as some thermophysical properties, assessed in ovendry condition: heat of combustion, J/kg, ash fraction, mass density, kg/m^3, specific heat capacity, J/kg K, and thermal conductivity, W/m K. For each category also must be specified an ignition temperature and a "pyrolysis temperature" (a hypothetical temperature at which solid fuel is converted to char and gaseous pyrolyzate) which is used to approximate the pyrolysis process as simple sublimation.

Other data required are the intensity (power per unit area, kW/m^2) and residence time, s, of an igniting heat pulse, windspeed, m/s, at the top of the fuel bed, depth of the fuel bed, m, ambient temperature, °C, duff loading (dry mass per unit area, kg/m^2) and duff moisture fraction, time step size, s, and number of time steps to be simulated, and three dimensionless empirical parameters whose numerical values are the subject of this investigation.

It should be noted that inclusion of windspeed and fuel bed depth as input quantities may be misleading. The speed of the flow of flame gases across the cylindrical fuel elements is derived as the vector sum of the windspeed, assumed horizontal, and the buoyancy induced vertical speed at the top of the fuel bed. This representative speed is used in determining the rate of heat transfer from flame gas to fuel by forced convection. The far more important and direct influence of wind on the rate of burning of duff and surface fuels is not modeled. Implicitly, calm conditions are presumed to exist and model sensitivity to windspeed is minimal.

Once the data described above are input, the surface fuel categories are sorted in order of increasing size, moisture content, and density. Then the loading of each category is parsed into components that are deemed to be interacting with other categories in its own size class and smaller ones, and with no other surface fuel elements. Note that the number of components in each category is the number of "smaller" size categories than itself plus two. The parsing depends upon the value of a parameter that is proportional to the product of the volume per unit area of the smaller category and the surface/volume ratio of the larger category whose loading is being parsed. The constant of proportionality is one of the empirical constants whose value is to be fixed (see discussion of fuel category partitioning below).

Once each surface fuel category's loading is thus distributed into interacting pairs, the simulation begins. A steady heat pulse of specified intensity and duration, such as the "reaction intensity" and "residence time" of a surface fire available as output from the BEHAVE system of fire behavior prediction models (Andrews 1986, Andrews and Chase 1989), is applied to the site. From this specified intensity, a fire environment temperature is derived and used to characterize the rate of heat transfer to the surface fuel components. The duff is presumed to commence burning at the end of the igniting heat pulse exposure, if its moisture content is less than about 200%.

The response of each surface fuel component to the igniting heat pulse is calculated in terms of the time required for its elements' outer surfaces to achieve ignition temperature. Sound fuels typically ignite at about 600 K, while rotten fuels may ignite at 550-575 K. Each component whose elements achieve ignition is classified as "lit" and its rate of burning is calculated from the rate of heat transfer to an element of that component and the heat required to raise an element unit volume to "pyrolysis temperature", including vaporization of its moisture content. If no components are lit during the ignition pulse, the simulation stops with that information displayed.

At the end of the ignition pulse period, the simulation-control clock is set to the duration of the ignition pulse but all event times kept internal to the simulation are reset so that the origin of time for the fuel components corresponds to the instant at which the first surface fuel component ignites. Among other events, the event of burnout of each surface fuel component is forecast and updated during each time step. When the internal clock reaches the time currently forecast for a fuel component to be totally consumed, the component is classified as "out". This means that components of the finest fuel categories may be "out" by the end of the ignition pulse period.

The simulation proceeds by marching time forward. At the beginning of each time step, the diameter reduction rate and dry mass loading reduction rate (burning rate) of each component is available from the previous time step. Also available is the time at which each component ignited (or is predicted to become ignited), at which it burned out (or is predicted to burn out) or at which it stopped burning because its local fire environment temperature fell too low. The model uses these burning rates to compute the rate of heat release per unit area — fire intensity — for the burn site as a whole, and the local rate of heat release per unit area for each fuel component. The local intensity is calculated as the sum of the site-average intensity and an incremental intensity computed for each component. The local intensity due to the burning of any given component is computed as the rate of heat release by that component per unit of burn site area *divided by the fraction of the burn site area occupied by that component*. Subtracting from this quantity the rate of heat release per unit of burn site area for the component, to avoid double counting, yields the *incremental local intensity* for that component. When this incremental local intensity is added to the site-average intensity, the result represents the local fire intensity that would be experienced by the interaction partner of that burning component.

For each time step, the model examines each surface fuel category, component-by-component. Based on the fraction of each category's loading that is currently burning, a "mixing parameter" is calculated

and used, along with the local fire intensity, to compute a local fire environment temperature. Two empirical constants are used in computing the mixing parameter (see "fire environment temperature" discussion below). The best choice of values for these parameters is determined by matching model predictions of laboratory wood crib burning rates to experimental data, as described below.

The fraction of each surface fuel category loading that does not interact with any other surface fuel element is assumed to interact with duff. The rate of duff burning is modeled as that of smoldering peat (Frandsen 1991a), so is fixed by its moisture content. This burning gives rise to a fire intensity contribution (Frandsen 1991b) that is added to the site-average intensity to determine the fire environment temperature for the affected surface fuel components. Duff burning is presumed to continue until a certain fraction of the total duff loading on site has been consumed. This fraction is computed using an empirical equation that depends only on the average moisture content of the duff layer (Brown et al 1985; Brown, Reinhardt, and Fischer 1991). No attempt is made to modify this fraction to account for possible interaction with burning surface fuels.

The local fire environment temperature is used to calculate the rate of heat transfer to an element of each fuel component to derive its diameter reduction rate and hence its mass loss rate. In the process the projected burnout times are updated as well as the ignition times for components not yet ignited. By summing over all the burning components, the site-average fire intensity is calculated, along with the incremental fire intensity for each fuel component.

The simulation proceeds until the specified number of time steps have been taken, until all surface fuel components have ceased burning or been consumed, or until the site-average fire intensity due to surface fuel burning falls below a preset minimum value of 0.1 kW/m^2. After the completion of each time step the simulation will, if the user desires, archive the current state of the burn site in terms of the remaining gross and dry total loading and the site-average fire intensity. If desired, this archival output can be expanded to include the dry loading and rate of change of same, diameter and diameter reduction rate, and time of start of surface drying, ignition, and "burnout" for each surface fuel component. At the end of the simulation, a summary of the residual loadings and diameters of each of the surface fuel components can be created. For each entry is also given the initial loading, moisture content, and ignition and burnout times.

In summary, the model simulates the burning process by calculating the rate of heat transfer to an element of each fuel component, based on its environment as characterized by the applicable fire environment temperature. This temperature depends upon the local fire intensity and a "mixing parameter" which in turn depends upon the fractions of each of the interacting fuel categories that are currently burning. From the rate of heat transfer, the diameter reduction rate for each fuel component is calculated, and thus its loading loss rate. The loading loss rate, along with the ash fraction and heat of combustion, gives its contribution to the site average fire intensity as well as to the local intensity, and thus the model is closed.

Fire Environment Temperature and Heat Transfer Rate

As discussed by Albini and Reinhardt (1995), the term "fire environment temperature" represents the temperature of an inert object residing in a steady fire environment that has attained equilibrium between the rates at which heat is transferred to and from the object. In the steady fires created by a propane burner in their laboratory experiments, this temperature was measured using a thermocouple embedded in a cement sphere of sufficient thermal mass that it required two to three minutes to achieve its ultimate steady temperature once placed in the flame. In a field situation, the local fire environment may change so rapidly that such an instrument could not be used successfully. Nevertheless, the concept can profitably be used if the fire environment temperature is understood to be the temperature that such an instrument would achieve in the local fire environment if that environment were to remain unchanged for a time of the order of a minute.

Thus interpreted, this temperature, T_F, can be used to characterize the rate of heat transfer to or from a fuel component exposed to the fire. The net heat transfer rate per unit surface area, q_{net}'', is modeled as the sum of convective and radiative heat transfer rates to a fuel element whose surface temperature is T_s, using an effective film heat transfer coefficient, h_{eff}:

$$q_{net}'' = h_{eff} (T_F - T_s) \qquad (1)$$

This heat transfer rate is averaged over the recent past, up to a specified maximum number of time steps, to obtain a representative value for each fuel component. Using this formulation, the time required for the surface of each fuel element to reach ignition temperature and the rate at which it burns are modeled, using simplified transient temperature response models and energy conservation relationships.

It should be noted here that the maximum number of time steps over which the fuel element heating rate running averages are determined is a parameter that can influence model operation and performance, as is the length of the time step. Model exercises with time steps between 5 and 30 *s* have been carried out, with little sensitivity noted, but good performance and smoothly varying burning rates seem to be achieved with a time step of about 10 *s*. The maximum number of time steps over which the heating rate running average is maintained has been fixed at 20 for all the trials done to date. This means that heating rate averaging spans between 100 and 600 *s* long have been used, with the great majority of exercise done with 200 *s* running averages. This time span seems appropriate and was selected purposely, and the user is cautioned that large excursions from the tested ranges of these quantities could cause unexpected model behavior.

The burning rate of a fuel element is derived from its rate of diameter reduction. The diameter reduction rate is modeled as the ratio of the current running average heat transfer rate to the heat required to raise a unit volume of the fuel from ambient condition to the pyrolysis temperature (which is also taken to be the fuel element surface temperature while it is burning), including vaporization of the moisture content of the fuel. Heat transfer modeling is described in more detail in Albini and Reinhardt (1995). For the present purpose we note that the local fire environment temperature is pivotal in establishing the ignition time delay and the rate of burning of fuel components. The sensitivity of this quanitity to empirical constants provides a means of determining the best values for them.

For a fire in natural fuels, we wish to characterize the fire environment for the burn site as a whole, and locally for pairs of interacting fuel elements (the components of each fuel category). In natural fires we are dealing conceptually with rather large actively burning areas. We presume that, for the fire intensity it supports, the area is too large to produce a single merged flame. Instead, the structure breaks into many distinct smaller flaming areas (Heskestad 1991). We deal with the whole burning area on an average basis by the artifice of assuming that there is a balance between the site-averaged fire intensity and the average rate at which heat is transferred away from the surface of the fire site.

The flame fluid flow convects heat away from the surface at the rate Q_c'' W/m^2. And heat is radiated away from the surface at the rate Q_r'' W/m^2. We assume both of these rates to be established by the fire environment temperature T_F. The rate of heat transport by upward-flowing hot products of combustion is

$$Q_c'' = \rho\, U\, C_p\, (T_F - T_a)\,, \qquad (2)$$

where ρ is the mass density of the fluid, U its mean upward velocity, C_p its specific heat capacity at constant pressure, and T_a is ambient temperature. Note that there is also downward flow of ambient air to replace the fluid flowing upward, but we assume this replacement air to be at temperature T_a and therefore to transport no excess heat. The radiation contribution to the heat loss rate is given by

$$Q_r'' = \varepsilon\, \sigma\, (T_F^4 - T_a^4)\,, \qquad (3)$$

where ε is the effective area-averaged integrated emissivity referred to the plane at which the temperature T_F is defined, and σ is the Stefan-Boltzmann constant = 5.67×10^{-8} $W/m^2\,K^4$. The sum of Q_c'' and Q_r'' should equal the fire intensity, I,

$$Q_c'' + Q_r'' = I\,. \qquad (4)$$

The rate at which solid fuel is turned to gaseous combustion products must be proportional to fire intensity divided by average heat of combustion, so

$$\rho\, U = (1 + \Phi)\, I / H_c \qquad (5)$$

where Φ is average air/fuel mass ratio and H_c average heat of combustion.

Using equations (2) - (5) to express the relationship between T_F and I gives the form

$$\theta = 1 + r / (1 + A\, r\, (\theta + 1)(\theta^2 + 1) / I) \qquad (6)$$

where

$$\theta = T_F / T_a\,, \qquad (7)$$
$$A = \varepsilon\, \sigma\, T_a^4\,, \qquad (8)$$

and

$$r = H_c / ((1 + \Phi)\, C_p\, T_a) \qquad (9)$$

is a parameter that depends on the mixture ratio of air to gaseous pyrolyzate. Clearly this number will be small when the area as a whole is characterized, but will be larger if attention is focused on the flame from two fuel elements burning very close to each other. If $\varepsilon = 1$, A is about 0.4 kW/m^2. To account for noncontinuous area coverage by flames and the fact that flame emissivity is less than unity, A is arbitrarily fixed in the model at 0.05 kW/m^2.

Figure 1 shows the modeled variation of T_F with I for a representative range of values of r. The maximum value of r is estimated to be about 2.5 for burning in still air. In the model r is composed of two parts, which are determined empirically. Note that there is a finite maximum temperature for a fire of infinite intensity:

$$max(\ T_F\ )\ =\ (\ 1 + r\ )\ T_a, \qquad (10)$$

so if T_a is 300 K and r is 2.5, the maximum fire environment temperature is 777° C, a value that is representative of flames from intense compartment and crib fires (Hasemi and Tokunaga 1983).

The simulation model uses equation (6) both for site-average fire environment temperature and for a temperature representing the local environment of interacting fuel elements. The values of I and r are adjusted in each case, in order to achieve the following sensitivities:

1. The minimum value of the mixing parameter, $r0$, is realized when a fuel element is not ignited and does not interact with a burning partner.
2. The maximum value of the mixing parameter, $r0 + dr$, is realized when a fuel element is ignited and interacts with a burning partner.
3. An ignited fuel element not interacting with a burning partner should have an intermediate mixing parameter value, $r0 + dr/2$.
4. Local fire intensity is computed in an expected value sense. Its minimum value is the site-average fire intensity, I_f, to which is added, as appropriate, site-average intensity due to duff burning, I_d, or incremental intensities from burning of the target element and/or its interaction partner.

Table 1 exhibits the rules for computing local fire intensity and mixing parameter values for determining local fire environment temperature. The incremental local fire intensity values are computed from the burning rates for each category, divided by the fraction of the burn site area covered at least once in effective planform area by fuel of the category in question.

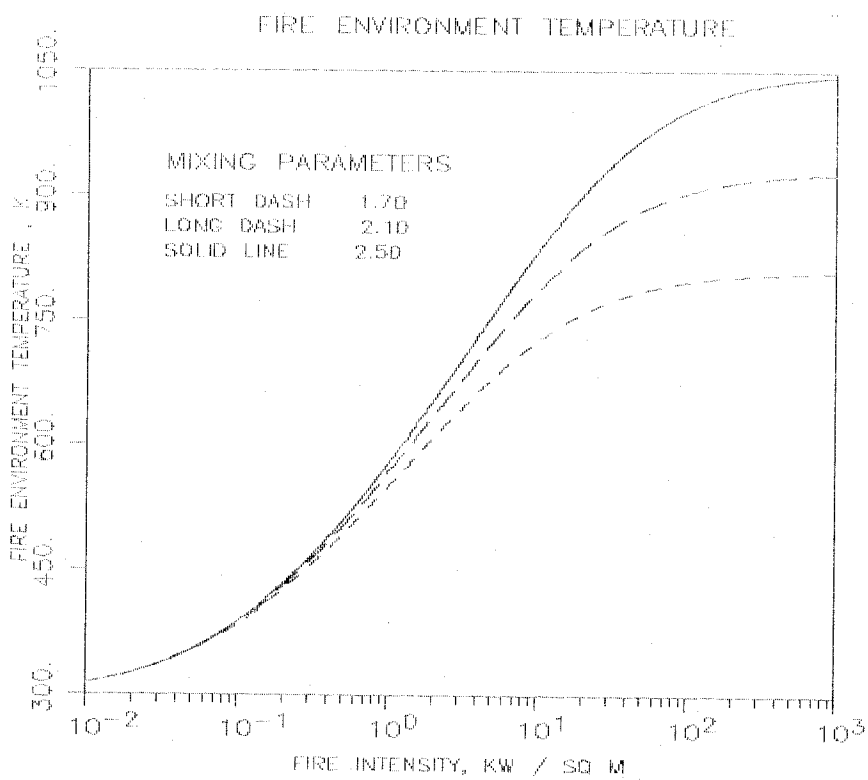

Figure 1. Fire environment temperature variation with fire intensity for several values of the "mixing parameter" r (see equations 6-9).

Table 1. Rules for selection of mixing parameter and calculation of local fire intensity. I_f is the site-average fire intensity, I_d the site-average intensity due to duff burning, and I_j, I_k are incremental local intensities due to burning of interacting fuel elements of categories j and k. Fuel component k, j of category k is being considered in this table. If the interaction partner category (j) of this component is ignited, it contributes an incremental intensity I_j to its local fire environment with probability f_j.

Case	Component ignited?	Size category of interaction partner	Fraction partner category ignited	Mixing parameter r	Local fire intensity I
1	No	None	—	r_0	$I_f + I_d$
2	No	Own = k	0	r_0	I_f
3	No	Smaller = j	f_j	$r_0 + 0.5 f_j dr$	$I_f + f_j I_j$
4	Yes	None	—	$r_0 + 0.5 dr$	$I_f + I_d$
5	Yes	Own = k	f_k	$r_0 + 0.5(1+f_k) dr$	$I_f + f_k I_k$
6	Yes	Smaller = j	f_j	$r_0 + 0.5(1+f_j) dr$	$I_f + I_k + f_j I_j$

Estimation of this fraction is based on the following idealization: Each fuel category is assumed to be composed of very many individual elements, each of which has a planform area (length X diameter) that is very small compared to the burn site area over which they are randomly strewn. The fuel element planform area is multiplied by a dimensionless constant K_a and the result is called the "effective planform area", assumed to represent a planform area of influence for each fuel element of the category. Calculation of the area fraction covered and the role of the dimensionless parameter K_a are discussed in the following section.

Fuel Element Interaction Partitioning

Partitioning of the loading of each surface fuel category into fractions interacting with other surface fuel categories or with no others is done at the beginning of the simulation and is not repeated as smaller size components burn out. Because of this aspect of the model, some of the larger sized fuel elements will often be predicted to be burned out more rapidly when they interact with their own size class than when they interact with smaller sizes. This occurs because the smaller sizes burn out, leaving their larger sized interaction partners to burn at reduced local intensities and with smaller mixing parameter values (and hence at lower fire environment temperatures).

The partitioning algorithm proceeds through the list of fuel categories in order of increasing size. In partitioning category i, all size categories from 1 through i are considered. The quantity b_{ij}

$$b_{ij} = K_a \, \sigma_j \, w''_i \, / \, \rho_i \, \pi \qquad (11)$$

is computed for each i, j pair using the empirical constant K_a. Here σ_j is the surface area/volume ratio of category j, w''_i the dry loading of category i, and ρ_i the ovendry mass density of fuel category i.

When j is less than i, j represents a smaller size category than does i and b_{ij} can be regarded as the product of the effective planform area per unit area of category i, multiplied by the ratio of the diameters D_i and D_j

$$b_{ij} = (D_i / D_j) \, b_{ii} \qquad (12)$$

and so b_{ij} can be interpreted heuristically as the maximum fractional diameter reduction of the loading of fuel elements of category i by elements of category j. The parameters b_{ij} are next constrained to be at most unity

$$b_{ij} = \min(1 , b_{ij}) \qquad (13)$$

and the list of fuel components is reexamined for the final partitioning.

For the final partitioning of fuel category i into interaction components, the sum of the quantities b_{ij} from $j = 1$ to i is formed. Call this sum B_i. If B_i is less than unity, then the b_{ij} values are taken to be the partition fractions for the loading of category i, and the difference (1 - B_i) is taken to be the fraction of the category not interacting with any other surface fuel. If the sum B_i exceeds unity, then B_i is used to normalize the b_{ij} values which are then used for the partitioning, and the fraction not interacting with any other surface fuel is taken to be zero.

Note that b_{ij} is equal to K_a times the planform area per unit of site area for fuel elements of size j. Recognizing this as the total "effective planform area" of fuel elements of size category j, and assuming the total to be the result of distributing many small contributions, it was shown in Albini (1976) that the expected fraction of the area covered at least once in

effective planform area by fuel elements of size class j is approximately β_{jj}, where

$$\beta_{jj} = 1 - \exp(-b_{jj}). \qquad (14)$$

The quantity βjj is used to compute the incremental contribution to the fire intensity due to burning of ignited category j components.

Note the behavior of the partitioning for limiting values of the empirical parameter K_a. If K_a grows large, all the b_{ij} values become unity. In this limit, the partitioning of fuel loadings is uniform over all categories of the same or smaller size and is independent of the empirical parameter. On the other hand, if K_a is small, all the b_{ij} values become small and proportional to K_a. In the limit of vanishingly small K_a, the fuel elements cease to interact. At an intermediate level such that the b_{ij} values are appreciable fractions of unity but do not exceed it, the sum B_i can exceed unity, and the renormalized partitioning can again become largely independent of the value of K_a. The partitioning in this case becomes proportional to the volume per unit area of the various categories.

In the old BURNOUT model (Albini 1976) this partitioning was used, but the b_{ij} values were interpreted, unrealistically, to be proportional to the loading of size category i that was burned out by interaction with category j. This interpretation is logically inconsistent with the assignment of burning times to the categories that can differ by more than an order of magnitude, and it makes predictions of fuel consumption strongly dependent upon the empirical parameter K_a. The present model strives for physical simulation of the fire environment and derives fuel consumption on that basis, so it eliminates the logical inconsistency and lessens model sensitivity to the parameter K_a, but the fuel interaction partitioning algorithm remains somewhat unsatisfying.

Burning Rate Calibration

As can be seen from the formulations above, no single parameter controls the prediction of the rate of fuel consumption by the model. While it is apparent that increasing $r0$ and/or dr would lead to prediction of higher fire environment temperatures (see Figure 1) and hence to more rapid fuel burning, the effect on burning rate of a change in the value of the area factor K_a is not readily apparent. The value of K_a influences the partitioning of the fuel categories into interacting component pairs, but, as described above, the variation of partition fractions is neither monotonic with nor overly sensitive to K_a.

To calibrate the model's prediction of burning rates, we relied upon an extensive set of wood crib burns conducted under controlled conditions at the Intermountain Fire Sciences Laboratory (Anderson 1990). In these experiments, dimensioned lumber cribs were burned under no-wind conditions while being continuously weighed, and gross weight was recorded as a function of time. Ignition was achieved by including poplar excelsior (long filaments of wood) in each crib and lighting a small quantity of a liquid hydrocarbon in a pan under the crib. The maximum weight loss rate occurred almost always within the first ten minutes, and this quantity was the focus of the original investigation.

The objective of the set of experiments was to discern the influence of various factors in controlling maximum burning rate, especially the exposed fuel surface area and the vertical vent area of the crib (Harmathy 1972ab, Drysdale 1985). Therefore some cribs were constructed with the intention of having their burning rates controlled by their vertical vent areas, some were constructed to exhibit burning rates controlled by exposed fuel surface area, and some were constructed with the intention of having the two areas about equally important in controlling the burning rates (see Tables 2, 3). The present model is designed for natural fuel accumulations and so should apply only to the cases where the exposed fuel surface area would control the burning rate. It should predict too high a burning rate when applied to the cribs with vertical vent area control.

We modeled the burning of the cribs using various values for the mixing parameters $r0$ and dr and using several values of the area factor K_a. For the igniting heat pulse we assumed that the excelsior burned completely in 20 seconds, and used its loading and heat of combustion to derive the intensity of the ignition pulse. Predictions of gross weight as a function of time were compared graphically and subjectively to measured data and a set of parameters was selected that afforded the "best" match to all the data except that from the cribs with burning rates controlled by vertical vent area. In the process of this subjective parameter selection, it was established that the area factor K_a had little influence on predicting the rate of burning, but the parameters $r0$ and dr were quite influential, as expected.

Figure 2 illustrates the sensitivity of predicted burning rate to the values of $r0$ and dr for crib HEALP21, one of the moderately loaded (at 300 T/ha!) cribs with burn rate controlled by exposed fuel surface area. The predictions were made using a value of 2.50 for K_a. The values 1.83 and 0.40 were selected for $r0$ and dr respectively, after examining a very large number of such graphs.

Table 2. Characteristics of the laboratory wood cribs whose burning rates were used to select the best mixing parameters r0 and dr for the simulation.

Burn Number	Dry Fuel Weight, kg	Fraction Excelsior	Fraction 1/4 in	Moisture Fraction
Cribs With Burning Rates Limited by Fuel Surface Area Exposed				
HEALP41	32.1	.00825	.0444	.060
HEAPP41	32.1	.00848	.0482	.067
HEALP21	44.1	.00720	.0431	.065
HEASF21	45.7	.00695	.0416	.065
HEALP31	51.3	.00531	.0353	.065
HEADF21	57.4	.00712	.0420	.065
HEAPP31	61.4	.00296	.0289	.060
HEASF41	72.0	.00692	.0422	.060
HEA2T111	78.3	.00973	.0913	.060
HEALP51	98.9	.00550	.0367	.060
HEAPP61	102.1	.00444	.0307	.060
HEADF41	103.4	.00702	.0378	.060
HEAPP101	106.5	.00681	.0341	.080
HEA2T061	159.3	.00683	.111	.060
HEAPP71	161.5	.00444	.0307	.060
HEA3T131	199.6	.00496	.0363	.060
Cribs With Burning Rates Initially Limited Equally by Top Surface Vent Area and by Fuel Surface Area Exposed				
HEAPP21	46.3	.00686	.0420	.060
HEADF31	81.1	.00279	.0291	.060
HEA3T161	81.2	.00559	.0392	.050
HEADF51	152.4	.00324	.0260	.137
HEADF52	152.4	.00324	.0260	.220
HEA3T151	188.7	.00461	.0331	.050
Cribs With Burning Rates Limited by Top Surface Vent Area				
HEASF31	82.0	.00205	.0230	.117
HEALP61	95.9	.00180	.0235	.225
HEASF51	161.0	.00176	.0206	.060
HEAPP81	163.7	.00298	.0241	.060
HEAPP91	217.7	.00204	.0213	.060
HEA3T141	235.0	.00399	.0269	.060
Cribs With Burning Rate Limits Not Determined				
HEA1T014	3.5	.0284	.227	.060
HEA3T171	23.9	.0830	.236	.060
HEA1T015	25.5	.0375	.241	.060
HEA3T173	25.5	.0781	.222	.060
HEA3T172	28.3	.0703	.200	.060

Using these subjectively "best" values for $r0$ and dr, a series of crib burns were simulated for area factors K_a between 0.05 and 2.5, to explore sensitivity to this factor. Results are shown in Figure 3 for the lightest (HEA1T014), the heaviest (HEA3T131), and an intermediate weight crib (HEALP21) for the extreme values of K_a used. From these figures it appears that the two values for the area factor give predictions of burning rate about equally satisfactory, but that an intermediate value might do better. These experiments represent exceptionally dry fuels at extremely high loadings. The lightest crib, HEA1T014, has a loading of 190 T/ha; the heaviest, HEA3T131, about 1350 T/ha.

To establish the best value for the area factor K_a, we turn to data on the consumption of natural fuels, as described in the next section. In doing so we are assured that the value of K_a selected will have very little effect on the quality of the predictions of burning rates for the laboratory cribs.

Surface Fuel Reduction Calibration and Test Data

Keeping the values of $r0$ and dr fixed, predictions of woody surface fuel loading reductions were made for various values of the area factor K_a, using preburn and postburn fuel inventory data taken during prescribed fire research studies. Predictions were compared to measured surface fuel reductions, and the value of K_a yielding the best agreement between predictions and measurements was sought. For this purpose, a calibration set of about half the available data was chosen randomly. A value for K_a was chosen to give good agreement between predictions and obser-

Table 3. Distributions of fuel size categories for the laboratory wood cribs used in burning rate calibration trials. Crib Fuel Loading Distributions by Size: Excelsior Plus Square Cross Section Dimensioned Lumber (Dimensions in Inches)

Burn Number	Excelsior	Loading, kg (Dry Weight) / m^2 1/4 x 1/4	1 x 1	2 x 2	4 x 4	6 x 6
HEA1T014	.437	4.30	14.1			
HEA1T015	.644	4.13	12.4			
HEA2T061	.732	11.9	30.9		63.6	
HEA2T111	.513	4.79	13.5	33.9		
HEA3T131	.668	4.89	14.1			115
HEA3T141	.632	4.27	12.5			141
HEA3T151	.586	4.21	12.3		110	
HEA3T161	.305	2.14	8.54	43.6		
HEA3T171	1.34	3.81	11.0			
HEA3T172	1.34	3.81	13.9			
HEA3T173	1.34	3.81	12.0			
HEADF21	.275	1.62	5.61	31.1		
HEADF31	.166	1.73	6.01	51.5		
HEADF41	.532	2.86	8.97		63.4	
HEADF51	.397	3.18	9.94		109	
HEADF52	.397	3.18	9.94		109	
HEALP21	.214	1.28	4.33	23.9		
HEALP31	.191	1.27	4.30	30.2		
HEALP41	.532	2.86	8.97		52.1	
HEALP51	.436	2.91	9.08		66.8	
HEALP61	.121	1.58	5.44	60.1		
HEAPP101	.488	2.44	7.72			61.0
HEAPP21	.214	1.31	4.55	25.1		
HEAPP31	.133	1.30	4.55	39.0		
HEAPP41	.239	1.36	4.78	21.8		
HEAPP51	.465	2.56	9.74		57.0	
HEAPP61	.363	2.51	7.77		71.1	
HEAPP71	.763	3.63	11.1			93.1
HEAPP81	.430	3.48	10.6			130
HEAPP91	.326	3.39	10.1			146
HEASF21	.214	1.28	4.49	24.8		
HEASF31	.118	1.32	4.57	51.5		
HEASF41	.483	2.94	9.36		57.0	
HEASF51	.206	2.42	7.60		107	

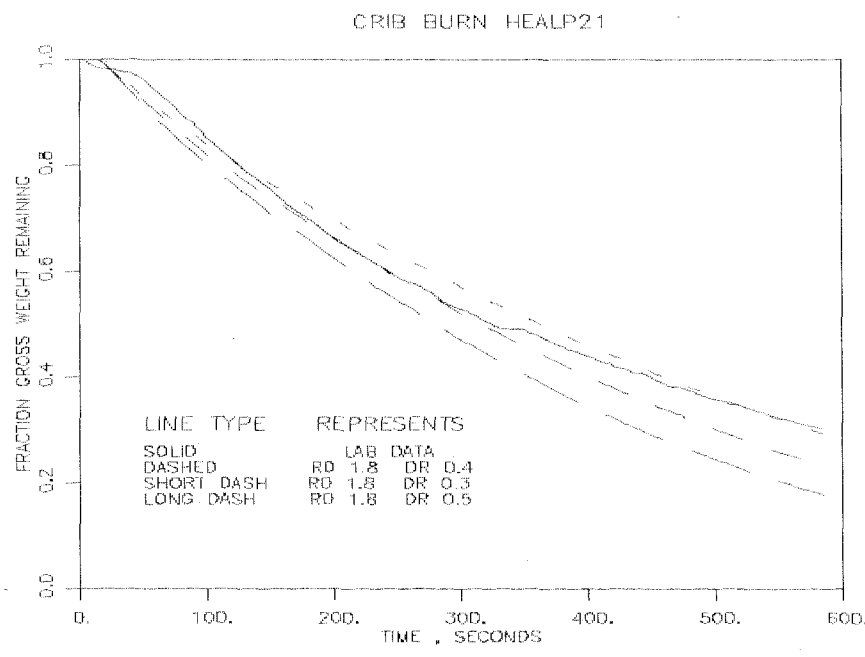

Figure 2. Predicted burning rates for crib HEALP21 for $r0 = 1.8$ and three different values of dr, compared to the experimental record of weight as a function of time. By means of many such graphical comparisons, the "best" values of $r0$ and dr, 1.80 and 0.43 respectively, were selected.

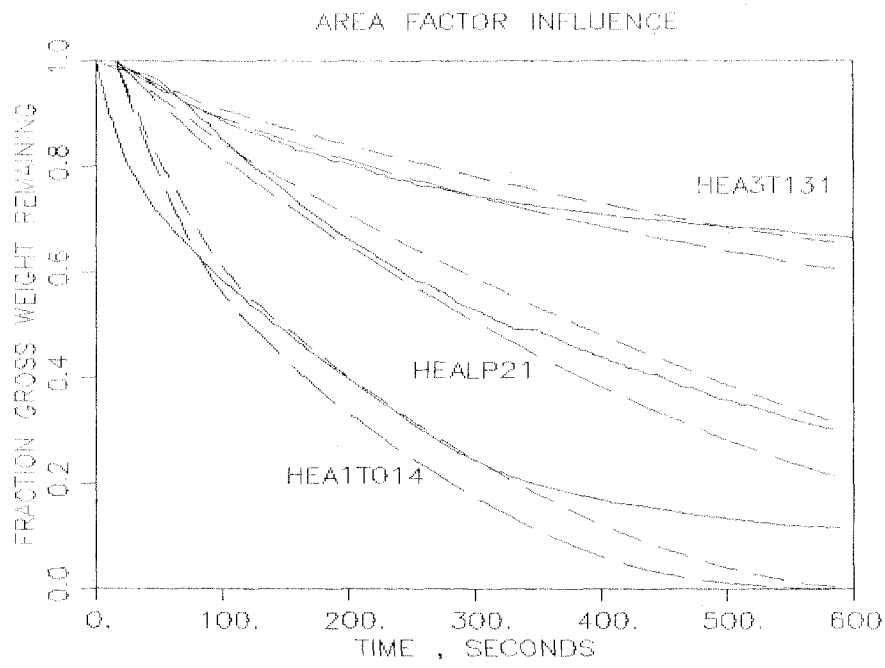

Figure 3. Weight vs time (solid lines) for a 3.5 kg crib, HEA1T014, a 44 kg crib, HEALP21, and a 200 kg crib, HEA3T131. Model predictions using area factors $K_a = 2.50$ (long dash) and 0.05 (short dash), and the "best" values for $r0$ and dr are shown for comparison.

vations of surface fuel reduction. Then the remaining data were processed in the same fashion and the performance of the model was evaluated against this test set. The data for calibration and test of the model came from three sources:

1. Twenty prescribed burns were carried out in natural fuel accumulations at the University of Montana's Lubrecht Experimental Forest as a doctoral thesis research project (Norum 1975). These data are identified by the shorthand designation "Lubrecht" below.

2. Thirty six plots in mixed conifer logging slash in northern Idaho were burned over a period of three years for research on fuel reduction by prescribed burning (Reinhardt, Brown, Fischer, and Graham 1991). These are identified as "Deception Creek" data, for the drainage in which the study was carried out.

3. A series of prescribed burns in logging slash was conducted over a period of several years for various research purposes, by workers at the USDA Forest Service Pacific Northwest Research Station; a broad selection of these burns had data stored in machine-readable format and were made available for use here. These data are identified as "PNW" in what follows.

Each data set includes preburn and postburn inventories of surface fuels and characterization of the duff loading and moisture content. Thermophysical properties (e.g., density, thermal conductivity, specific heat capacity, etc.) were not measured, so representative handbook values were used for these parameters. The character of the igniting fire was not quantified in any of the studies, but it is clear from the fact that a loading reduction was measured for each burn unit that some large surface fuel was ignited and consumed by fire in every case. A set of preliminary model exercises led to the selection of an ignition pulse of 50 kW/m^2 for 60 s (representing the burning of about 0.15 kg/m^2 of kindling fuels) which was sufficient to ignite at least some large surface fuels on all sites.

Nonuniformity of fuel loading can give rise to considerable variation in fuel consumption, especially if ignition effort is concentrated to any degree on fuel accumulations of greater than average loading when burning conditions are marginal. Migration of large fuel elements during burning also takes place. Fuel elements that roll downhill and leave the inventory transect show up as consumed totally by fire, while elements that move onto the transect can appear as an

anomolous increase in fuel loading. In this study, surface fuel loading increases in any size class were treated as zero reductions. Such confounding effects are characteristic of field research on wildland fire, and must be accepted as sources of variability.

Each data set has also some unique features which need to be considered in interpreting the calibration and test computations. Some unique aspects of the data sets are outlined and their implications in the present context are discussed below.

Deception Creek

Fuels were the result of recent logging in a decadent stand. Rotten fuels were both preharvest and activity fuels, while sound fuels were mostly activity fuels. Sites were steep, and fuel loadings were high.

Preburn and postburn fuel loadings were measured on the same twenty permanently marked transects, using the planar intersect technique. Small diameter, 1/4 - 1 (6.35 - 25.4 mm) and 1 - 3 inch (25.4 - 76.2 mm), pieces were counted on six foot (1.83 m) and ten foot (3.05 m) transects, respectively, while larger pieces were recorded by diameter and sound/rotten classification on 50 foot (15.24 m) transects. Unit average preburn and postburn loadings were computed by size class from the transect data, and consumption was computed as the difference between the two. In a few cases, "negative consumption" was computed for one or more size classes, probably as a result of pieces rolling onto the transect, or larger pieces being partially consumed and being counted in a smaller class in the postburn inventory. We assume that this sampling error is small, that pieces rolling onto the line are offset by pieces rolling off, and that the effect of pieces changing size classes disappears when size classes are totaled to estimate total fuel consumption for a unit. For the Deception Creek data, the magnitude of these negative values was small — an average of 0.8% of preburn loading.

In this study series, 60 logs were more intensively measured on each of 18 units. Moisture content and diameter reduction were measured for each log. The moisture contents were summarized by size class and sound/rotten. These are the moistures used for calibration here. The diameter reduction data showed a lot of variability so we did not use them here.

The Deception Creek data are unusually complete in scope. Surface fuel loadings were inventoried for fuels as small as 1/4 - 1 inch in diameter, and 0 - 1/4 inch loadings were estimated using samples collected from small areas to establish representative relative loadings of 0 - 1/4 and 1/4 - 1 inch components. Fuels were characterized as sound or rotten and large fuel moisture contents were measured for 18 units. Duff loading and moisture content samples were extensive and the study provided abundant duff reduction measurements from spikes.

The surface fuel consumption data from this set are thorough and thought to be quite reliable. The moisture content range of the larger surface fuels was large, being 32 - 61% (sound) and 50 - 111% (rotten), but most of the fuels under 1 inch (25.4 mm) in diameter were at about 10% moisture content and the litter-derived duff (over the whole study area) was rather shallow and quite dry. Because of these features, the simulation sees each of the sites as readily ignitable, but the range of duff burning influence on surface fuel consumption is rather restricted. Strip headfires up the 50-80% slopes were lit by propane torches to ignite these burns.

The eighteen units with complete fuel moisture data had an average preburn surface fuel loading of 13.9 kg/m^2 and an average surface fuel loading reduction of 6.75 kg/m^2 49%), with a coefficient of variation of 1/3. The loadings are relatively large for current harvest and utilization practice, but the fractional reduction by burning is not and the unit-to-unit variation is rather small.

Lubrecht

The Lubrecht Experimental Forest burns were carried out in older fuel accumulations under standing timber on slopes varying from steep to nearly flat and, on average, not as steep as at Deception Creek. Fuels included natural fuels and debris from a harvest approximately 50 years earlier.

Woody fuels were inventoried using techniques similar to those applied at Deception Creek. Thirteen sampling planes were used in each unit. Two meter transects were used to tally fuels less than three inches (76.2 mm) in diameter, and four meter transects for larger fuels. As at Deception Creek, preburn and postburn loadings were computed from transect data by size class and consumption was taken to be the difference between the two.

The problem of "negative consumption" was more evident than in the Deception Creek data. In addition to rolling and changing size classes, some Lubrecht transects gained fuels when standing trees fell on them. This did not occur in the Deception Creek data because the burn units were clearcuts or residual trees were very large. Of 20 units burned at Lubrecht, 19 had an increase in loading in at least one size class, and one unit had a total postburn fuel loading greater than the preburn loading.

The biggest contributor to negative fuel consumption appears to be fuels that were tallied as rotten in the preburn inventory and as sound in the postburn inventory. The increases in loading ascribed to the sound classes were treated by our data processing rules as being zero reductions. But the imputed "total consumption" of those rotten components that changed classification is not discernible in the data. The effects of this aberration (which occurred in 13 - 17 of the 20 burns) are that the loading reductions of sound components are understated and those of rotten components overstated. So, if the model worked flawlessly, it would be deemed to have overpredicted consumption of large sound fuels and to have underpredicted large rotten fuel consumption. As "partly rotten" components are not currently modeled, there is no way accurately to account for their effects.

Total surface fuel loadings were relatively light compared to the harvest debris burns, averaging 6.23 kg/m^2 for the 20 units. Large fuel moisture content was not measured for these burns, but were measured for fuels up to 1 inch in diameter. We used the measured moisture content of the 1/4 - 1 inch fuels for the 1 - 3 inch fuels, and the reported values (Norum 1975, 1976) of the calculated National Fire Danger Rating 1000 hr fuel moisture content for the larger components.

Duff loadings and moisture contents were sampled for each site and the fuel inventory data are considered to be accurately sampled. The burns all seem to have been carried out under moist conditions. In almost every case, the smaller size fuels whose moisture contents were measured had significantly higher moisture contents than were computed for the 1000 hr timelag components. Loadings of 0 - 1/4 inch and 1/4 - 1 inch fuels for these sites were much smaller fractions of the 1 - 3 inch and larger loadings, probably because these were mostly natural fuel accumulations rather than debris from recent harvests. The relatively light loadings of these "kindling" fuels hints that ignition may have occurred nonuniformly on some sites, in local concentrations of surface fuels.

PNW

Data from this extensive set of experimental burns in harvest debris revealed some consistent differences between fuels and burning conditions on the dry interior sites of the Deception Creek and Lubrecht studies and the more moist sites of Western Washington and Oregon. Unlike the Deception Creek and Lubrecht studies, the sites in the PNW study are broadly distributed geographically and in terms of forest type and harvest method. Surface fuel moisture contents were measured. The differences are no doubt real and stem from the soil, climate, and species differences between the two locales.

Preburn fuels were sampled using planar transect methods, with a total transect length of 4000 feet 1.219 km) per site (Sandberg and Ottmar 1983). Consumption of large woody fuels was estimated not from postburn transects, but from average diameter reductions of a set of 20 - 40 pieces that were banded with wire before and after burning. Moisture content was measured on the pieces that were wired. Quadratic mean diameter was computed for each size class of preburn large fuels based on the transect data, then diameter reduction was applied to this to estimate average postburn diameter. Because of this methodology, "negative consumption" was never observed. The samples to be wired were selected from sound, cured pieces with preburn diameters between three inches (76.2 mm) and 12 inches (304.8 mm).

The physical sizes of the fuel components were larger in the PNW data, but the loadings were not. The mean loading of surface fuels for the PNW burn sites was 7.30 kg/m^2, which is much closer to the Lubrecht natural setting data (6.23 kg/m^2) than to the atypically heavy harvest debris of Deception Creek (13.9 kg/m^2). The duff loadings on the PNW sites were considerably greater than on the Deception Creek sites and less than on the Lubrecht sites, but the PNW duff was typically much more moist than that on either of the interior locale sites. The large sound fuels in the PNW burns were also much more moist than those on either of the other study areas. The combined effects of moist duff and moist large surface fuels led to the smallest mean surface fuel consumption, 3.85 kg/m^2, which is less even than the Lubrecht study average of 4.53 kg/m^2.

The PNW surface fuel consumption data exhibited very little variation from site to site; the standard deviation of surface fuel loading reduction was 1.72 kg/m^2 compared to 2.25 for Deception Creek and 2.46 for Lubrecht. The reason for this consistent difference is not apparent. A contributing factor might be the omission of rotten fuel components from PNW inventories taken before and after each fire, but this was not felt to be a significant omission since rotten fuels contributed but a small fraction of the surface fuel loadings. But because the variance in surface loading reduction is so small, the influence on loading reduction of various factors thought to be pertinent is difficult to discern and even more difficult to test quantitatively.

Table 4. Results of calibration exercises of the simulation to predict fuel consumption in prescribed burns in three locales. Mean and standard deviation of surface fuel loading reductions are given in kg/m^2, along with mean errors of prediction and mean squared errors of prediction in the same units.

				K_a				
				0.6	1.2	1.8	2.4	3.0
Study area	Burns	Load Reductions Mean	Load Reductions Std Dev	Mean errors of prediction / Mean squared errors of prediction				
Deception Creek	8	5.63	1.98	-0.19	0.02	0.20	0.36	0.50
				1.54	1.16	1.00	0.97	1.02
Lubrecht	10	4.88	2.84	-0.25	-0.17	-0.10	-0.03	0.03
				1.11	1.01	0.94	0.89	0.87
PNW	15	4.06	1.36	1.40	1.49	1.58	1.67	1.75
				5.18	5.61	6.10	6.58	7.05
Lubrecht & Deception Creek	18	5.21	2.53	-0.23	-0.09	0.03	0.14	0.24
				1.30	1.08	0.97	0.93	0.94
All Sources	33	4.69	2.16	0.51	0.63	0.74	0.84	0.93
				3.06	3.14	3.30	3.50	3.72

Model Calibration and Test

Eight sites from the Deception Creek data set, ten from Lubrecht, and 15 from PNW were selected randomly for calibration trials. Predictions of surface fuel loading reduction were made for each of the sites, for a range of values of the empirical area factor parameter K_a from 0.6 to 3.0, using an ignition pulse of 50 kW/m^2 for 60 *s*. This ignition pulse was found by trial and error to be minimally sufficient to ignite at least some large surface fuel on each burn site. The energy density of this ignition pulse is 3 MJ/m^2, which would be released by burning of about 0.15 kg/m^2 of kindling fuel. This quantity of fuel is available on every plot in the data set, as part of the loading of litter and 0 - 1/4 inch diameter surface fuels. Such fuels would be almost completely consumed in about one minute after first ignition at any point, so the modeled ignition pulse is not excessively energetic.

Table 4 shows the results of this calibration trial for each of the three study areas, for Deception Creek and Lubrecht combined, and for all three study areas combined. The Deception Creek and Lubrecht data, considered separately and in combination, are very well predicted by the model, as judged by the fact that the mean square error of prediction is small compared to the variance of the data and that the minimum mean square error occurs near zero mean error of prediction. The PNW data are poorly predicted by the model, with the mean square error of prediction exceeding the variance of the data. In other words, the model does not predict the variation in the data as well as using a constant prediction equal to the mean of the data.

These observations are quantified by the data presented in Table 5. This table exhibits measures of the degree to which the model predictions fit the data of the calibration set. The quality of this fit can be judged in several ways. If one were dealing with a predictive model that relied upon input data which had no uncertainty (hence, whose predictions were numerically certain) one could simply perform a linear regression of the measured (and therefore somewhat uncertain) surface fuel loading reductions against the model's predictions and use the familiar coefficient of determination (r^2) as a single measure of the fidelity of the model. Additional measures of the quality of the fit of observations to predictions are given in Table 5 in the form of linear functions that would "best" describe scatter plots of the observations against the model predictions.

Fits are of the form $y = a + bx$ and $y = cx$, where x is total surface fuel reduction model prediction and y is measured reduction. Fits are found by determining the values of a and b, or of c, which place the line nearest, in the least mean square sense, to all the point pairs (x,y) in light of the fact that both x and y are subject to errors of measurement. The y values are differences between two experimental measurements, while the x values each depend nonlinearly upon a set of measured quantities. Clearly an "accurate" model would result in a small value (compared to the mean of the observations) for a, and values for b and c near unity. But if such quantities are obtained it does not follow that the model is accurate, but only that its predictions show little bias. It is the variation of these

Table 5. Measures of the degree to which model predictions fit measurements of surface fuel loading reduction for three prescribed burn study locales. The second column gives values of a measure of model error, defined to be 1 - (mean squared error of prediction) / (variance of observations). Parameters a and b are intercept and slope of a least squares best fit of a straight line graphing observations against predictions. Parameter c is the slope of the same best fit line if it is constrained to pass through the origin.

Study area	Burns	K_a	1 - MSE/VAR	Linear fits to scatter plots a	b	c
		0.60	0.609	-5.39	2.03	1.08
Deception		1.20	0.706	-4.25	1.75	1.04
Creek	8	1.80	0.746	-3.62	1.59	1.00
		2.40	0.754	-3.20	1.47	0.97
		3.00	0.741	-2.88	1.39	0.95
		0.60	0.863	-0.56	1.18	1.08
		1.20	0.875	-0.54	1.15	1.06
Lubrecht	10	1.80	0.884	-0.50	1.13	1.04
		2.40	0.890	-0.48	1.10	1.03
		3.00	0.892	-0.45	1.09	1.01
		0.60	-1.800	1.61	0.45	0.71
		1.20	-2.032	1.64	0.44	0.70
PNW	15	1.80	-2.297	1.68	0.42	0.68
		2.40	-2.557	1.73	0.41	0.67
		3.00	-2.811	1.76	0.40	0.66
		0.60	0.796	-1.24	1.29	1.08
Lubrecht &		1.20	0.831	-1.13	1.24	1.05
Deception	18	1.80	0.848	-1.04	1.19	1.02
Creek		2.40	0.854	-0.96	1.15	1.00
		3.00	0.853	-0.89	1.12	0.98
		0.60	0.342	-0.42	0.98	0.91
		1.20	0.325	-0.35	0.95	0.89
All Sources	33	1.80	0.290	-0.26	0.91	0.87
		2.40	0.247	-0.19	0.88	0.85
		3.00	0.200	-0.12	0.86	0.84

linear fit parameters with the empirical factor K_a, and their consideration in conjunction with the mean and mean square errors of prediction, that yield the modeling insights sought. The interpretation we see in the variation of these fitting parameters with K_a is as follows:

1. The Deception Creek data can be predicted accurately by proper choice of K_a value; strong sensitivity of a and b to choice of K_a and the shallow minimum of mean square error near K_a = 2.4 indicates a small number of poorly predicted units, with the predictions being sensitive to the value of K_a.

2. The Lubrecht data are well predicted by the model and the predictions are insensitive to the value of K_a used. There is a trend toward slightly better predictions as K_a increases, continuing even at K_a = 3, but there is little improvement to be achieved.

3. The PNW data show a substantial bias that is only weakly sensitive to the value of K_a and this dependence is in the opposite sense to that of the Lubrecht data. This implies that there are some number of units whose fuel reductions are badly overpredicted by the model, that the predictions depend only weakly upon the value of K_a and predictions increase as K_a increases.

Detailed analysis of the individual burn unit results for the various data sets confirms these interpretations. A pleasantly surprising finding from the detailed assessment was that a large majority of the PNW burn units were in fact accurately predicted by the model, but that five were substantially overpredicted. This is visually apparent from a comparison of the scatter plots in Figures 4 and 5. Figure 4 is a scatter plot of predicted and measured surface fuel loading reductions from the calibration set of burn units from the Deception Creek and Lubrecht study sites, with the predictions made using K_a = 2.4. In Figure 5, data from 15 PNW sites are added. Note the five units that appear in the lower righthand corner of this plot.

The pattern of these two figures is repeated for the other values of K_a used in the first set of calibration trials. The loading reductions seem to be predicted either very accurately or rather inaccurately. No reason for the inaccurate predictions was apparent in the data, and the predictions are only weakly sensitive to the value of K_a used. But the errors arising from these few burns (15% of the calibration set) forced the calibration of the area factor to the range of quite small values. The second set of calibration trials used a K_a range of 0.10 - 0.50 leading us to the selection of K_a = 0.4 as the best compromise value. Clearly a value near 2.4 would better fit the data from Deception Creek and Lubrecht, but a smaller value than 0.10 would be needed to optimize performance against the PNW data, as is apparent from the entries in Table 6.

As with all field data, there are bits of anecdotal information that "explain" some observations. For example, one of the PNW sites for which the model badly overpredicted fuel consumption endured rain for 45 minutes right after ignition. This we discovered while seeking reasons for the large errors of prediction for some sites. But as no search was made to explain very accurate predictions, this discovery is not a research finding but an anecdote.

To minimize one source of misprediction, the duff moisture contents for all units were artificially adjusted to the values that would cause the model to predict the observed duff consumptions. This adjustment reduced the bias (mean error of prediction) by about 1/4 and the rms error of prediction by about 1/3 for the PNW data,

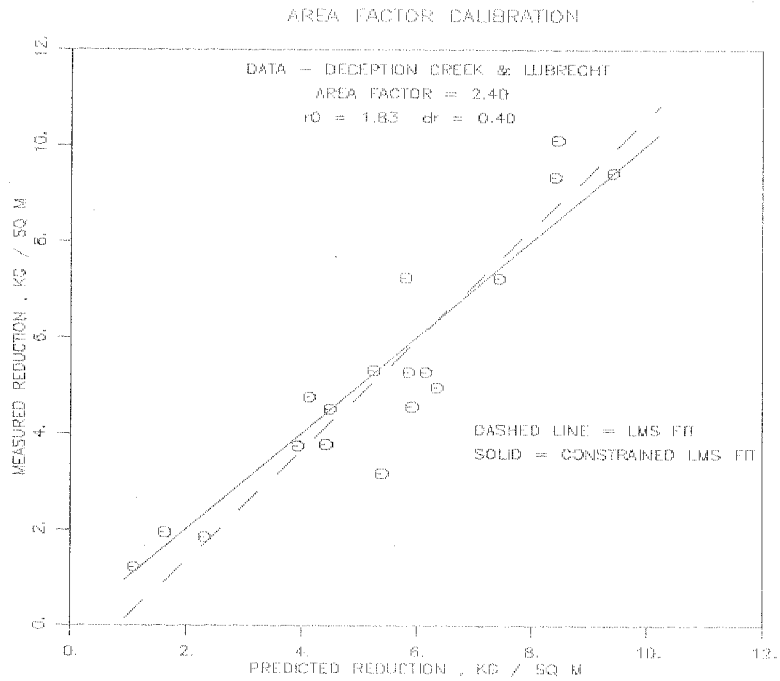

Figure 4. Scatter plot of calibration exercise predictions and measurements of surface fuel loading reductions for 18 burn sites from data sets for Deception Creek and Lubrecht study areas. Two least squares linear fits are shown; the solid line is constrained to include the origin; the dashed line is not.

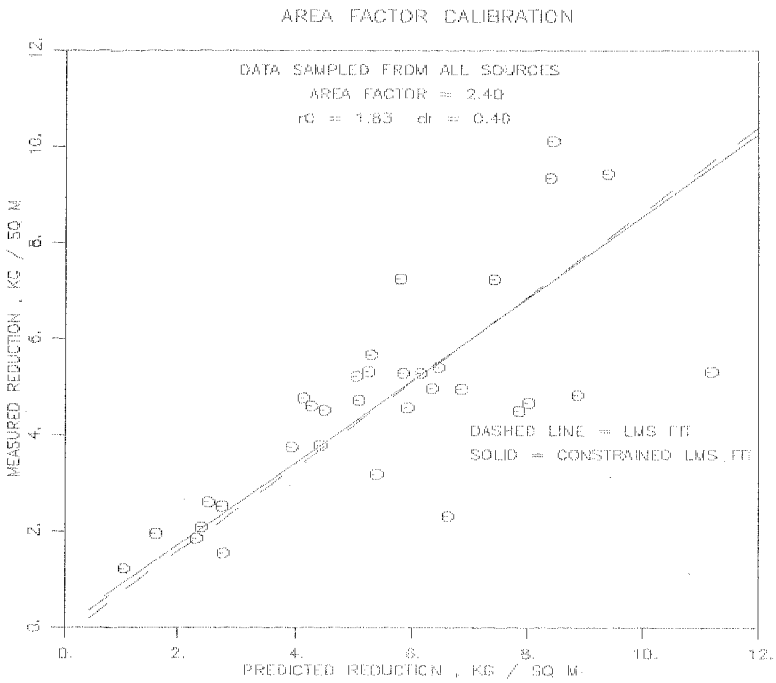

Figure 5. Scatter plot of Figure 4 with the addition of 15 burn sites from PNW study areas. Note the five severe overpredictions now included.

Table 6. Presents the same measures of the degree to which model predictions fit measurement data for selection and test of area factor as in Table 5, but using only data not included in the calibration trials (second block) and using all data (last four blocks). The range of values for K_a is much smaller in this table than in Table 5 also.

Study area	Burns	K_a	1 - MSE/VAR	Linear fits to scatter plots a	b	c
		0.10	0.338	0.46	1.01	0.93
Calibration		0.20	0.340	-0.45	1.00	0.93
data set -	33	0.30	0.342	-0.45	1.00	0.92
all sources		0.40	0.342	-0.44	0.99	0.92
		0.50	0.342	-0.43	0.99	0.91
Test set		0.10	0.648	-0.74	1.10	0.98
(all data		0.20	0.646	-0.71	1.08	0.97
excluded	37	0.30	0.643	-0.68	1.07	0.96
from		0.40	0.643	-0.65	1.06	0.96
calibration)		0.50	0.640	-0.62	1.05	0.95
		0.10	0.411	-2.67	1.56	1.14
Deception		0.20	0.431	-2.58	1.53	1.13
Creek	18	0.30	0.451	-2.49	1.50	1.12
		0.40	0.468	-2.43	1.48	1.11
		0.50	0.484	-2.35	1.46	1.10
		0.10	0.825	-0.68	1.15	1.03
		0.20	0.825	-0.68	1.14	1.02
Lubrecht	20	0.30	0.827	-0.67	1.14	1.02
		0.40	0.827	-0.67	1.14	1.02
		0.50	0.828	-0.66	1.13	1.02
		0.10	-0.229	0.77	0.62	0.75
		0.20	-0.253	0.78	0.62	0.75
PNW	32	0.30	-0.273	0.79	0.61	0.74
		0.40	-0.294	0.80	0.61	0.74
		0.50	-0.317	0.80	0.61	0.74
		0.10	0.531	-0.66	1.07	0.96
		0.20	0.531	-0.64	1.06	0.95
All Data	70	0.30	0.529	-0.61	1.05	0.94
		0.40	0.529	-0.59	1.04	0.94
		0.50	0.528	-0.57	1.03	0.94

but had almost no influence on the prediction errors for the other data, for $K_a = 0.4$. While the adjustment was beneficial where it was expected to have been, it did not dramatically reduce the largest errors. But it is encouraging that the accuracy of predictions improved when a source of error was suppressed.

Figure 6 shows the scatter plot of measurements versus predictions for the calibration data set and Figure 7 shows the same for the data that were not used in the calibration trials. This scatter plot appears to show better agreement between measurements and predictions than was achieved for the calibration data. This observation is confirmed by the numerical measures of model performance given in Table 6.

Figure 8 is a scatter plot of measurements versus predictions of surface fuel loading reduction for the entire data set, using 0.4 for the value of K_a. Different symbols are used for the data from the three different study areas in Figure 8, allowing one to discern visually the trends of overprediction for some units of the PNW data set and underprediction of a few units of the Deception Creek data set, with the Lubrecht data clustering near the diagonal line of perfect agreement.

Summary

A simulation model for the burnout of large natural fuels has been assembled and tested. The rate at which fuel elements burn is modeled as a balance between the rate of heat transfer to a burning fuel element and the energy required to heat a unit volume of the fuel to a hypothetical "pyrolysis temperature" at which the fuel sublimes. This artifice permits construction of a relatively simple model for the extraordinarily complex real process of pyrolysis and combustion of the gaseous and solid products.

Heat transfer is calculated as the sum of convective and radiative terms, driven by a "fire environment temperature" which is modeled as dependent upon the local fire intensity and a pair of empirical parameters that conceptually describe the amount of excess air mingled with combustion products in the flame fluid flow. These parameters control the prediction of burning rate, so numerical values for them were selected by fitting model predictions to measurements of laboratory wood crib burning rates.

The increase in local fire environment temperature when two fuel elements interact was maximal in the laboratory wood cribs, because they were so heavily loaded. For more lightly loaded natural fuel accumulations, the components interact only when they are in close proximity. The probability of such interaction between pairs of fuel components is modeled crudely as being proportional to the fraction of the burn site area that is covered at least once in planform projection by the "effective interaction area" for each pair of fuel components. This area includes an empirical factor that influences the ultimate amount of surface fuel consumption, but only weakly. Prescribed fire studies of surface fuel consumption provided data sufficient to calibrate and test this empirical factor. The numerical value selected for this parameter from this exercise is rather small, and there is evidence that model performance might be further improved by using a smaller value yet, but some ambiguity remains concerning the trend of model performance with this quantity.

The model includes the influence of duff burning on the consumption of surface fuels, by including the contribution of the burning duff to fire intensity for fuel components not interacting with other woody surface fuel. The amount and rate of duff consumption in the model depends upon its moisture content, but the

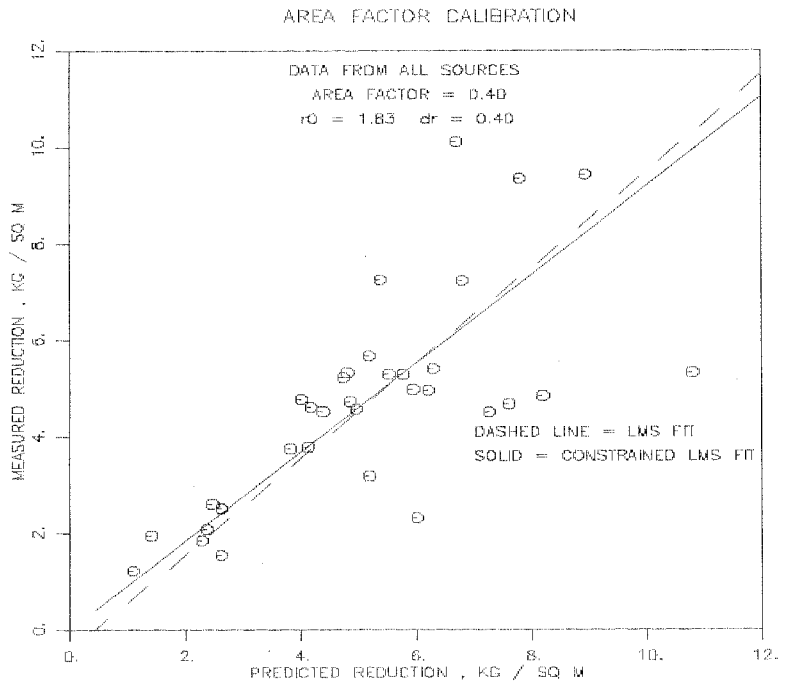

Figure 6. Area factor calibration exercise shows acceptable surface fuel reduction predictions using area factor 0.4 and data from all study areas.

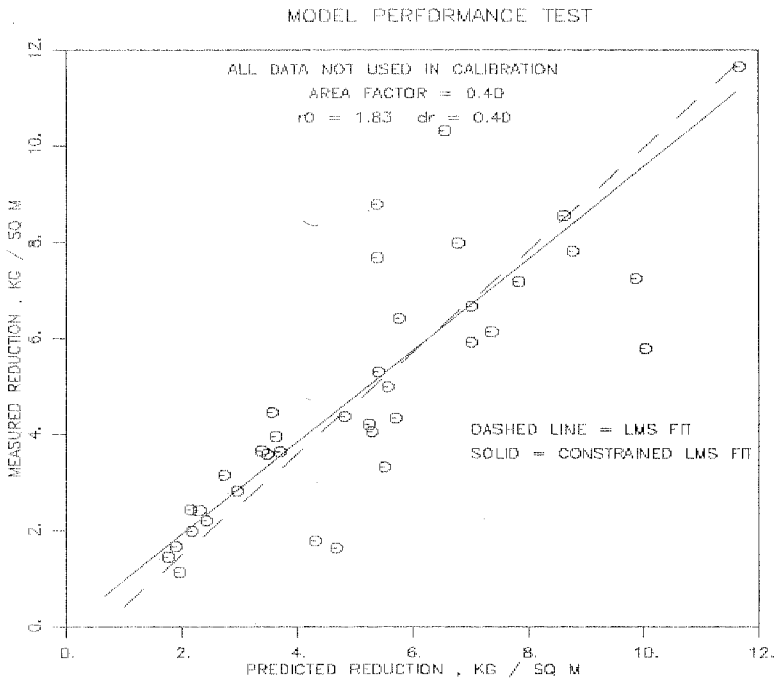

Figure 7. Performance of the model in predicting surface fuel loading reductions for all sites excluded from the calibration exercises.

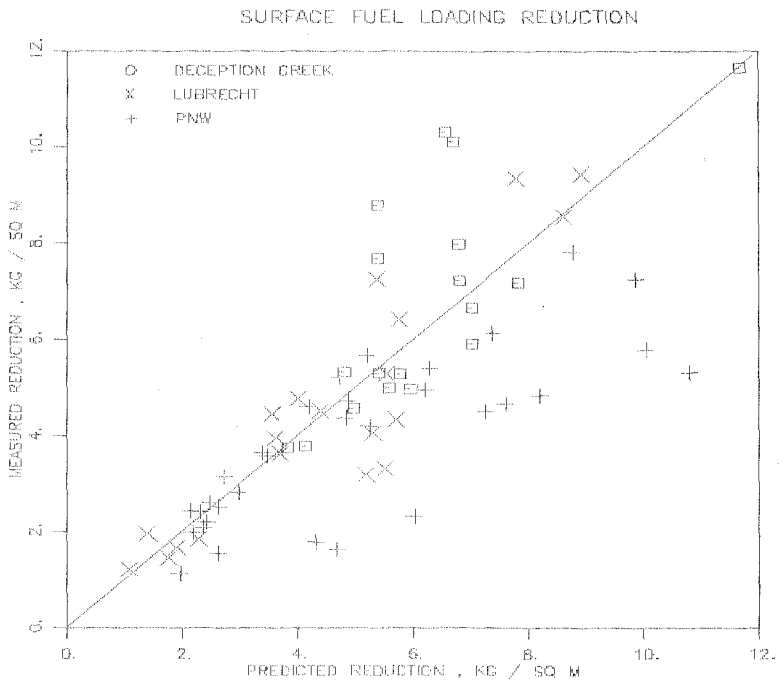

Figure 8. Scatter plot superposition of Figures 6 and 7, using different symbols for the three different study areas. Note underprediction of three Deception Creek units and overprediction of six to eight units from PNW data set.

important effect of wind on duff burning rate is omitted. This omission represents a major residual weakness of the model, and it should be used only to represent calm conditions until this deficiency is remedied.

Acknowledgement. The senior author gratefully acknowledges support of this research by USDA Forest Service, Intermountain Research Station, under research grant INT-92754-GR, and continuing sponsorship and collaboration under research joint venture agreement INT-94947-RJVA. We note with appreciation the special effort by Ms. Roberta Hartford, USDA Forest Service Intermountain Fire Sciences Laboratory, who found, resurrected, and interpreted the laboratory wood crib time series data for us. Critique of an early draft of this paper by Ms. Patricia Andrews, USDA Forest Service Intermountain Fire Sciences Laboratory, Mr. Mark Finney, Systems for Environmental Management, and Dr. Brad Hawkes, Canadian Forestry Service, Pacific Forestry Centre, was generously afforded and proved to be most helpful.

References

Albini, F. A., 1976: Computer-based models of wildland fire behavior: A users' manual. USDA Forest Service Unnumbered publication, Intermountain Research Station, Ogden UT. 68 pp.

Albini, F. A., 1981: Spot fire distance from isolated sources — extensions of a predictive model. USDA Forest Service Research Note INT-309, Intermountain Research Station, Ogden UT. 9 pp.

Albini, F. A., 1986: Wildland fire spread by radiation — a model including fuel cooling by natural convection. Combustion Science and Technology Volume 45, pp 101-113.

Albini, F. A., 1994: Program BURNUP, a simulation model of the burning of large woody natural fuels. Final report on USDA Forest Service Research Grant INT-92754-GR, Montana State University Mechanical Engineering Department. Unpublished report on file at USDA Forest Service Intermountain Fire Sciences Laboratory, Missoula MT.

Albini, Frank A., and Elizabeth D. Reinhardt, 1995: Modeling ignition and burning rate of large woody natural fuels. International Journal of Wildland Fire 5(2):81-91.

Anderson, Hal E., 1990: Relationship of fuel size and spacing to combustion characteristics of laboratory fuel cribs. USDA Forest Service Research Paper INT-424, Intermountain Research Station, Ogden UT. 9 pp.

Andrews, P. L., 1986: BEHAVE: Fire behavior prediction and fuel modeling system—BURN subsystem, part 1. USDA Forest Service General Technical Report INT-194. Intermountain Research Station, Ogden UT.

Andrews, P. L., and C. H. Chase, 1989: BEHAVE: Fire behavior prediction and fuel modeling system — BURN subsystem, part 2. USDA Forest Service General Technical Report INT-260. Intermountain Research Station, Ogden UT.

Brown, Arthur A., and Kenneth P. Davis, 1973: Forest fire: Control and use, 2nd edition. McGraw-Hill, New York, 686 pp. See chapters 6 and 7.

Brown, J. K., M. A. Marsden, K. C. Ryan, and E. D. Reinhardt, 1985: Predicting duff and woody fuel consumption in the northern rocky mountains. USDA Forest Service Research Paper INT-337, Intermountain Research Station, Ogden UT. 23 pp.

Brown, James K., Elizabeth D. Reinhardt, and William C. Fischer, 1991: Predicting duff and woody fuel consumption in northern Idaho prescribed fires. Forest Science, Volume 37 Number 6 pp 1550-1566.

Chandler, C., P. Cheney, P. Thomas, L. Trabaud, and D. Williams, 1983: Fire in forestry. Volume 1, Forest fire behavior and effects. Wiley-Interscience, New York.

Drysdale, Dougal, 1985: An introduction to fire dynamics. John Wiley and Sons, Chichester. 424 pp. See chapter 5.

Frandsen, William H., 1991a: Burning rate of smoldering peat. Northwest Science, Volume 65 Number 4, pp 166-172.

Frandsen, William H., 1991b: Heat evolved from smoldering peat. International Journal of Wildland Fire, Volume 1 Number 3, pp 197-204.

Grishin, A. M., 1981: Matematicheskoye modeli lesnykh pozharov (Mathematical models of forest fires), Tomsk State University Press, Tomsk. 277 pp (Russian)

Grishin, A. M., 1992: Matematicheskoye modelirovaniye lesnykh pozharov i novyye sposoby bor'by s nimi (Mathematical modeling of forest fires and new methods of fighting them), Nauka, Novosibirsk. 408 pp. (Russian)

Harmathy, T. Z., 1972a: A new look at compartment fires, Part I. Fire Technology Volume 8 Number 3, pp 196-217.

Harmathy, T. Z., 1972b: A new look at compartment fires, Part II. Fire Technology Volume 8 Number 4, pp 326-354.

Hasemi, Y., and T. Tokunaga, 1983: Modeling of turbulent diffusion flames and fire plumes for the analysis of fire growth, pp 37-46 In Quintierre, J. G., R. L. Alpert, and R. A. Altenkirch (editors), "Fire dynamics and heat transfer", Annals of American Society of Mechanical Engineers, Heat Transfer Division, HTD-Volume 25. ASME, New York, 138 pp.

Heskestad, Gunnar 1991: A reduced-scale mass fire experiment. Combustion and Flame, Volume 83, pp 293-301.

Hungerford, Roger D., 1990: Describing downward heat flow for predicting fire effects. Problem analysis, problem no. 1, addendum, 7/9/90, Research Work Unit FS-INT-4403, Fire effects: Prescribed and wildfire. USDA Forest Service Intermountain Research Station, Intermountain Fire Sciences Laboratory, Missoula MT. 100 pp.

Incropera, Frank P. and David P. DeWitt, 1985: "Fundamentals of heat and mass transfer", second edition. John Wiley & Sons, New York, 802 pp. Section 7.4.2.

Luke, R. H., and A. G. McArthur, 1977: Bushfires in Australia, Australian Government Publishing Service, Canberra, 359 pp. See Chapters 4 and 6.

Norum, Rodney A., 1975: Characteristics and effects of understory fires in western larch/Douglas-fir stands. Ph.D. dissertation, University of Montana School of Forestry, Missoula MT. 155 pp.

Norum, Rodney A., 1976: Fire intensity-fuel reduction relationships associated with understory burning in larch/Douglas-fir stands. pp 559-572 In: Proceedings Tall Timbers fire ecology conference no. 14 and Intermountain Fire Research Council fire and land management symposium, October 1974, Missoula MT. Tallahassee FL: Tall Timbers Research Station.

Reinhardt, Elizabeth D., James K. Brown, William C. Fischer, and Russel T. Graham, 1991: Woody fuel and duff consumption by prescribed fire in northern Idaho mixed conifer logging slash. USDA Forest Service Research Paper INT-443 Intermountain Research Station, Ogden UT. 22 pp.

Rothermel, R. C., 1972: A mathematical model for predicting fire spread in wildland fuels. USDA Forest Service Research Paper INT-115, Intermountain Research Station, Ogden UT. 40 pp.

Sandberg, D. V., and R. D. Ottmar, 1983: Slash burning and fuel consumption in the Douglas-fir subregion, pp 90-93 in: Seventh conference on fire and forest meteorology, American Meteorological Society, Boston MA.